

Impact of high-energy tails on granular gas properties

Thorsten Pöschel,¹ Nikolai V. Brilliantov,^{2,3} and Arno Formella⁴

¹Charité, Augustenburger Platz, 10439 Berlin, Germany

²Institute of Physics, University of Potsdam, Am Neuen Palais 10, 14469 Potsdam, Germany

³Department of Physics, Moscow State University, Vorobievsky Gory 1, 119899 Moscow, Russia

⁴Department of Computer Science, Universidad de Vigo, Edificio Politécnico, 32004 Ourense, Spain

(Received 22 March 2006; published 19 October 2006)

The velocity distribution function of granular gases in the homogeneous cooling state as well as some heated granular gases decays for large velocities as $f \propto \exp(-\text{const} \times v)$. That is, its high-energy tail is overpopulated as compared with the Maxwell distribution. At the present time, there is no theory to describe the influence of the tail on the kinetic characteristics of granular gases. We develop an approach to quantify the overpopulated tail and analyze its impact on granular gas properties, in particular on the cooling coefficient. We observe and explain anomalously slow relaxation of the velocity distribution function to its steady state.

DOI: [10.1103/PhysRevE.74.041302](https://doi.org/10.1103/PhysRevE.74.041302)

PACS number(s): 47.70.-n, 51.10.+y

When a homogeneous granular gas evolves in the absence of external forces, it develops a velocity distribution similar to that of a molecular gas; however, its temperature decays due to the dissipative nature of particle collisions. The velocity distribution function of granular gases has attracted much scientific attention since it deviates characteristically from the Maxwell distribution. There are two types of deviations. First, there are deviations from the Maxwellian in the main part of the distribution [1,2], where the particle velocities are close to the thermal velocity $v_T(t) = \sqrt{2T}$ (unit particle mass is assumed). Second, the high-energy part, $v \gg v_T$, deviates in its functional form, i.e., the distribution function decays as $f \propto \exp(-\text{const} \times v)$ [2,3], instead of $f \propto \exp(-\text{const} \times v^2)$ as expected for the Maxwell distribution. Heated granular gases with a Gaussian thermostat are equivalent to gases in the homogeneous cooling state (HCS) [4]. That is, the addressed properties apply for a wide class of granular gases. Figure 1 shows the velocity distribution function and its deviation from the Maxwellian (details see below).

Both types of deviations are characterized by the coefficient of restitution ε describing the postcollision particle velocities \vec{v}'_1 and \vec{v}'_2 as functions of the precollision velocities,

$$\vec{v}'_{1/2} = \vec{v}_{1/2} + [(1 + \varepsilon)/2](\vec{v}_{12} \cdot \vec{e})\vec{e} \quad (1)$$

with $\vec{v}_{12} \equiv \vec{v}_1 - \vec{v}_2$ and the unit vector $\vec{e} \equiv (\vec{r}_1 - \vec{r}_2)/|\vec{r}_1 - \vec{r}_2|$ at the moment of the collision.

In the HCS, the velocity distribution $f(\vec{v}, \tau)$ (where the time τ is measured in the average number of collisions per particle) can be reduced to a time-independent distribution function $\tilde{f}(\vec{c})$ by the transformation

$$f(\vec{v}, \tau) = (n/v_T^3(\tau))\tilde{f}(\vec{c}), \quad \vec{c} \equiv \vec{v}/v_T(\tau), \quad (2)$$

with Haff's law [5] for the temperature evolution,

$$dT/d\tau = -2\gamma T, \quad \text{i.e.,} \quad T(\tau) = T(0)\exp(-2\gamma\tau). \quad (3)$$

The main part of the distribution function, $c \sim 1$, can be described with good accuracy by a second-order Sonine polynomial expansion around the Maxwell distribution $\phi(c) \equiv \pi^{-3/2}\exp(-c^2)$:

$$\tilde{f}(c) = \phi(c)[1 + a_1 S_1(c^2) + a_2 S_2(c^2) + \dots]. \quad (4)$$

It can be shown that $a_1 = 0$; therefore, the leading deviations from the Maxwell distribution are due to the second Sonine polynomial $S_2(c^2) = c^4/2 - 5c^2/2 + 15/8$ and the respective coefficient a_2 [1,2,6]:

$$a_2 = 16(1 - \varepsilon)(1 - 2\varepsilon^2)/[81 - 17\varepsilon + 30\varepsilon^2(1 - \varepsilon)]. \quad (5)$$

The good agreement of Eq. (4) with simulation data in the region $c \sim 1$ can be seen in Fig. 1 (top).

For $c \gg 1$, Eq. (4) fails to represent the velocity distribution function due to its different functional form. It has been shown that for particles with high velocities the distribution function develops an exponential tail [2,3],

$$\tilde{f}(c) = B e^{-bc}, \quad b = 3\pi/\mu_2, \quad \mu_2 = \sqrt{2\pi}(1 - \varepsilon^2)\left(1 + \frac{3}{16}a_2\right), \quad (6)$$

which is illustrated in the bottom part of Fig. 1; here μ_2 is the second moment of the collision integral; see, e.g., [7].

The overpopulation of the tail is a rather general feature of granular gases: After being theoretically predicted [3], it was found for gases in the HCS also numerically [8,9] as well as for driven gases, and was also detected experimentally; e.g., [10–14]. In spite of its obvious importance, still it lacks a theoretical description that allows one to quantify its impact on granular gas properties. Indeed, neither the numerical prefactor B in Eq. (6) nor the threshold velocity above which the tail is overpopulated is known. In the present Brief Report we address this problem numerically and analytically. We develop an approach to quantify the high-energy tail and estimate its impact on gas properties. The impact of the tail on the cooling rate is studied in detail.

We perform direct simulation Monte Carlo (DSMC) [15–17] of $N = 10^8$ granular particles. The DSMC method is particularly suited to simulate large systems over long times in the HCS, that is, to suppress spatial correlations which give rise to vortices [18] and clusters [19]. We started at $T(0) = 1$ and simulated until the particle velocities approached the double-precision number representation, i.e., until $T \approx 10^{-23}$. For $\varepsilon = 0.9$ this corresponds to a total of 5×10^{10} collisions or 1000 collisions per particle. Neglecting

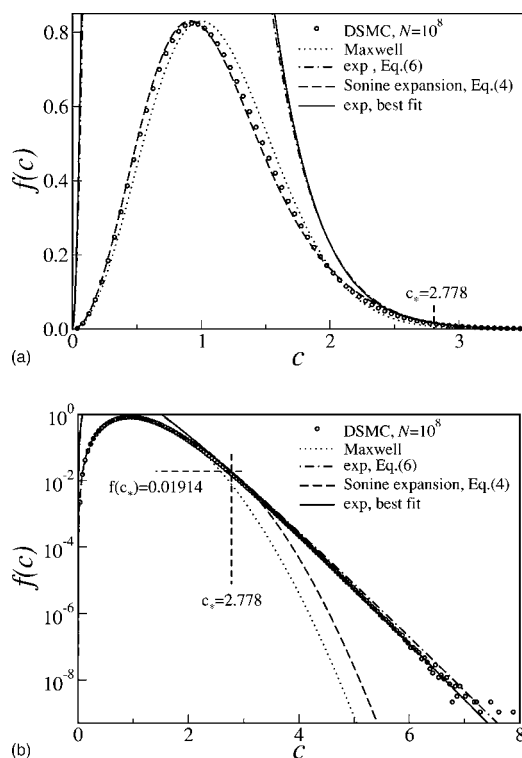


FIG. 1. Velocity distribution function of a granular gas $\tilde{f}(\tilde{c})$ as normal and logarithmic plot. The symbols show a simulation of $N = 10^8$ particles for $\varepsilon = 0.3$. For $c \sim 1$, $\tilde{f}(\tilde{c})$ is well described by the second-order Sonine expansion Eq. (4) (top). For comparison the Maxwell distribution is also shown. For $c \gg 1$ the distribution function decays exponentially slowly (bottom) [see Eq. (6)]. The tail starts at $c \approx c_*$, Eq. (9).

the first 2×10^9 collisions, after each 10^8 collisions (two collisions per particle) we recorded a snapshot of the scaled velocities c . The distribution function $\tilde{f}(c)$ was then obtained by binning of up to 100 of such snapshots in 100 intervals.

The numerical values of the constants B and b were then determined by performing a least-mean-square fit of the linear function $B' - bc$, where $B' = \log B$. To find the numerical value of the threshold velocity where the tail starts, c_* (see the discussion below) we discriminate between two cases. For the first case, where the functions $B \exp(-bc)$ and $\tilde{f}(c)$ according to the Sonine expansion Eqs. (4), (5) intersect, we determine c_* as the mean of the two intersection points; these were very close to each other in all our simulations. For the second case, where the functions do not intersect, c_* was determined as the scaled velocity that minimizes the distance between both functions. Such simulations were performed for $\varepsilon = 0.1, 0.2, \dots, 0.9$.

In Fig. 2 the numerical results for the slope b are compared with the theoretical prediction, Eq. (6). For $\varepsilon \leq 0.7$ we find good agreement, whereas for larger ε the data deviate. This can be understood from the theoretical argument used to derive $\tilde{f}(c) \propto \exp(-bc)$ [3,20]. For $c \rightarrow \infty$ the gain term of the Boltzmann equation may be neglected as compared with the loss term. The larger the restitution coefficient ε , the later the tail starts. In contrast, for molecular gases where $\varepsilon = 1$, the

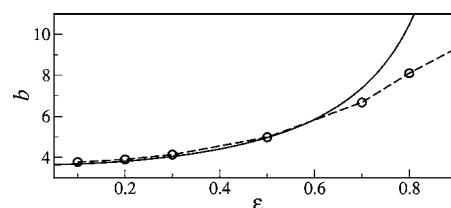


FIG. 2. The slope b of the exponential tail. For $\varepsilon \leq 0.7$ we find good agreement of the DSMC results with the theoretical expression given in Eq. (6) (full line). For smaller dissipation the data deviate (see text).

gain and loss terms balance each other for all velocities, leading to the Maxwell distribution $\tilde{f}(c) \propto \exp(-c^2)$. The deviation for $\varepsilon \gtrsim 0.7$ originates from the fact that the gain term cannot be neglected for large ε for the accessible interval of velocities.

To obtain the threshold velocity c_* analytically we assume that $f(c)$ may be sufficiently well described by a combination of Eq. (4), valid for $c \sim 1$, and Eq. (6) for the tail,

$$\tilde{f}(c) = Ac^2 e^{-c^2} [1 + a_2 S_2(c^2)] \Theta(c_* - c) + Bc^2 e^{-bc} \Theta(c - c_*), \quad (7)$$

with the Heaviside function $\Theta(x)$, i.e., we disregard the transient region [20] between the near-Maxwellian and exponential parts of the distribution. Using the DSMC method we checked the ansatz (7), whose eligibility is illustrated in Fig. 1 for $\varepsilon = 0.3$. The unknown parameters A , B , and the threshold velocity c_* may be found from the normalization condition and continuity of the distribution function itself and its first derivative

$$\tilde{f}(c_* + 0) = \tilde{f}(c_* - 0), \quad \tilde{f}'(c_* + 0) = \tilde{f}'(c_* - 0), \quad (8)$$

where $\tilde{f}' = d\tilde{f}/dc$. From normalization it follows that

$$c_* = b/2 + a_2(2c_*^3 - 5c_*)/2[1 + a_2 S_2(c_*^2)], \quad (9)$$

$$A^{-1} = [k(c_*)/b^3] [2 + bc_*(2 + bc_*)] e^{-bc_*} + (\sqrt{\pi}/4) \operatorname{erf}(c_*) - \frac{1}{8} c_* [4 + a_2 c_*^2 (2c_*^2 - 5)] e^{-c_*^2}, \quad (10)$$

$$B = Ak(c_*), \quad (11)$$

with

$$k(c_*) \equiv e^{-c_*^2 + bc_*} [1 + a_2 S_2(c_*^2)]. \quad (12)$$

Solving the fifth-order equation (9) numerically for c_* , we obtain A , k , and finally B (Fig. 3).

The very good agreement between simulations and the theoretical predictions for the coefficients $A(\varepsilon)$, $B(\varepsilon)$ and the transition velocity $c_*(\varepsilon)$ manifests the adequacy of the ansatz (7). The deviation for $\varepsilon \gtrsim 0.7$ occurs already for the slope b of the exponential tail (Fig. 2), and is not related to the ansatz. It may be explained similarly as the deviation of b from its theoretical value: For large $\varepsilon \gtrsim 0.7$ the system of $N = 10^8$ particles is not large enough to develop a well-detectable exponential tail.

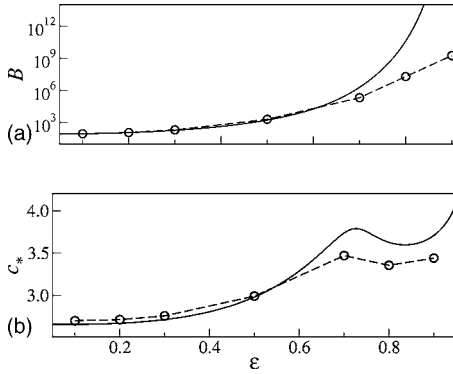


FIG. 3. The threshold velocity c_* and the parameter B as obtained from DSMC calculations (symbols) together with the solution of Eqs. (9) and (11). Again, for $\varepsilon \leq 0.7$ we find good agreement.

Knowing the distribution function Eq. (7) and its parameters A , B , and c_* as functions of ε , we can quantify the impact of the exponential tail on kinetic quantities. In this Brief Report we focus on the temperature decay rate γ ; for the diffusion coefficient, and other transport coefficients as well as for technical details we refer to [23].

The standard analysis (e.g., [2,7]) yields for the temperature decay rate, when the stationary velocity distribution is achieved

$$\gamma = (1 - \varepsilon^2)J_2/12J_0, \quad (13)$$

where

$$J_k = \int d\vec{c}_1 d\vec{c}_2 \int d\vec{e} \Theta(-\vec{c}_{12} \cdot \vec{e}) |\vec{c}_{12} \cdot \vec{e}|^{k+1} \tilde{f}(c_1) \tilde{f}(c_2). \quad (14)$$

Disregarding the exponential tail, the energy decay rate reduces to [2]

$$\gamma_0(\varepsilon) = (1 - \varepsilon^2)/6 [1 + (3/16)a_2(\varepsilon)] / [1 - (1/16)a_2(\varepsilon)]. \quad (15)$$

We applied the DSMC simulation of 10^8 particles for different ε and recorded the temperature $T_{\text{DSMC}}(\tau)$. Then γ_{DSMC} was determined by fitting $T_{\text{DSMC}}(\tau)$ for $\tau \gg 1$ to its asymptotic law, $T_{\text{DSMC}} \propto \exp(-2\gamma_{\text{DSMC}}\tau)$ [Eq. (3)]. Figure 4 (inset) shows $\gamma_{\text{DSMC}}(\varepsilon)$ (points) together with the analytical result, $\gamma_0(\varepsilon)$, Eq. (15) (line). In this representation we hardly see any discrepancy between theoretical and numerical data. The difference between these curves (main part of Fig. 4), which quantifies the impact of the overpopulated tail on the cooling rate reveals, however, a clear dependence on ε . The scaling law $\gamma_0 - \gamma_{\text{DSMC}} \propto \exp(-6\varepsilon)$, shown here only as a numerical result, is, however, difficult to confirm analytically: In spite of the simple functional form of $\tilde{f}(c)$, Eq. (7), an accurate analytical expression for the cooling coefficient may be obtained only in the limit $\varepsilon \ll 1$ [23]. As follows from the discussion below, the studied system of $N=10^8$ particles is not sufficiently large to analyze this limit by numerical simulations.

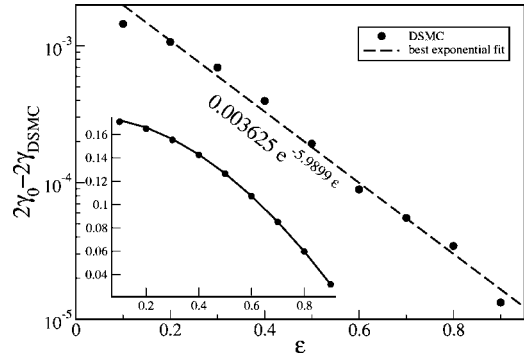


FIG. 4. Inset: The temperature relaxation coefficient $\gamma(\varepsilon)$ over ε as obtained by DSMC simulation, γ_{DSMC} , (points) and due to Eq. (15), γ_0 . The logarithmic plot shows $\gamma_0 - \gamma_{\text{DSMC}}$, that is, the influence of the exponential tail on the cooling coefficient. The dashed line shows the best exponential fit.

So far, the discussion refers to the state when the velocity distribution $\tilde{f}(c)$ has relaxed to its stationary form. Now we ask the question, how fast does this happen? To address this problem we initialize the particle velocities according to a Maxwell distribution at $T(0)=1$ and investigate the decay of temperature as a function of the average number of collisions, τ . Asymptotically, i.e., when the gas has adopted its asymptotic distribution, the temperature evolves according to Haff's law, Eq. (3). Thus, the time lag that is needed for a system to reach Haff's evolution corresponds to the relaxation time of the distribution function to achieve its stationary form $\tilde{f}(c)$.

Using the coefficient γ_{DSMC} described above, we define the temperature $T_{\text{fit}}(\tau) \propto \exp(-2\gamma_{\text{DSMC}}\tau)$. By definition, for $\tau \gg 1$ we have $T_{\text{DSMC}} \approx T_{\text{fit}}$ since γ_{DSMC} was determined as the best exponential fit to $T_{\text{DSMC}}(\tau)$ for $\tau \gg 1$. Therefore, the quantity $1 - T_{\text{DSMC}}(\tau)/T_{\text{fit}}(\tau)$ characterizes the relaxation of the distribution function to its stationary form. Figure 5 shows the relaxation for different values of the coefficient of restitution. We note that, depending on ε , the relaxation to the level of “natural” fluctuations in the system takes approximately 20–30 collisions per particle. This slow relaxation is very different from that in a molecular gas, where it takes very few (3–5) collision per particle to develop the Maxwell distribution. Similar slow relaxation of the high-

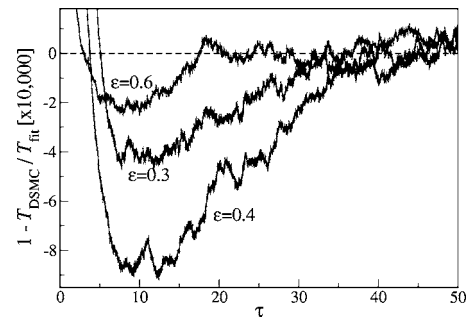


FIG. 5. Relaxation of the temperature decay to Haff's law for $N=10^8$ and $\varepsilon=0.3, 0.4, 0.6$, characterizing the relaxation of the distribution function to its stationary form.

energy tail of the velocity distribution was reported for a gas of elastic hard spheres [21]. The relaxation mechanism for the case of granular gases is, however, completely different and depends on ε : While the tail in elastic gases is fed by the gain term of the Boltzmann equation, for the dissipative gases this term is negligible. The formation of the tail for the latter case occurs exclusively due to permanent cooling of the gas, so that the scaled velocity of a particle, $\vec{c} \equiv \vec{v}/v_T$, increases due to decaying v_T . By this mechanism particles enter the tail and keep it overpopulated.

The relaxation time, i.e., the time of formation of the exponential tail, may be quantified. The relaxation to the stationary distribution $\tilde{f}(c)$ is described by [7,22]

$$(\mu_2/3)(3 + c \partial/\partial c)\tilde{f}(c, \tau) + J_0(\partial/\partial \tau)\tilde{f}(c, \tau) = \tilde{I}(\tilde{f}, \tilde{f}) \quad (16)$$

where $\tilde{I}(\tilde{f}, \tilde{f})$ is the reduced collision integral (e.g., [7]) and J_0 is defined in Eq. (14). Neglecting the incoming term for $c \gg 1$ [2–4], the collision integral may be approximated by

$$\tilde{I}(\tilde{f}, \tilde{f}) \approx -\pi c \tilde{f}(c), \quad c \gg 1. \quad (17)$$

Using the ansatz $\tilde{f}(c, \tau) = B \exp[-w(\tau)c]$, we recast Eq. (16) into

$$dw/d\tau + (\mu_2/3J_0)w = \pi/J_0, \quad c \gg 1, \quad (18)$$

with the solution

$$w(\tau) = b + (1 - b)\exp[-\pi\tau_0(\varepsilon)], \quad (19)$$

where $b = 3\pi/\mu_2$ coincides with Eq. (6) and $\tau_0^{-1}(\varepsilon) = \mu_2/3J_0$. Neglecting a_2 , which characterizes small deformations of the main part of the distribution with respect to the Maxwellian, and the contribution from the tail, we obtain $J_0 = 2\sqrt{2}\pi$ and hence

$$\tau_0^{-1}(\varepsilon) = (1 - \varepsilon^2)/6 \quad (20)$$

(see [23] for details). For $\varepsilon = 0.4$ we obtain the relaxation time, $\tau_0 \approx 7.1$.

Let us compare the theoretical prediction Eq. (20) with the numerical results. The relaxation of $(1 - T_{\text{DSMC}}/T_{\text{fit}})$ as plotted in Fig. 5 reveals two stages. First, for $\tau \leq 10$, we observe relaxation of the main part of the velocity distribution, where $c \approx 1$. The initial Maxwell distribution relaxes here to the distribution given by the Sonine expansion Eq. (4). During the second stage the overpopulated tail is formed; the plotted quantity decreases for $\varepsilon = 0.4$ by a factor of 10 in the time span $\Delta\tau = 25$ ranging from $\tau = 10$ to 35. This leads to a numerical relaxation time $\tau_0 = 25/\log 10 \approx 10.8$, in agreement with the above theoretical estimates.

The theory also predicts that the relaxation time increases with increasing ε . While this tendency is confirmed for $\varepsilon = 0.3$ and 0.4, it is seemingly violated for $\varepsilon = 0.6$ (see Fig. 5). We argue, however, that this is, presumably, a finite-size effect, which may be understood as follows. According to the mechanism of the tail formation, discussed above, the gain term of the collision integral does not contribute to the tail.

Instead, particles enter the tail due to increase of the scaled velocity $\vec{c} \equiv \vec{v}/v_T$ when the thermal velocity v_T decreases along with temperature T . The temperature decay and hence the formation of the tail is slower for larger ε , that is, the relaxation time τ_0 is larger, Eq. (20).

On the other hand, the total number of particles in the tail moving at velocities $c > c_*$, decreases with increasing ε . Correspondingly, the deviation of the distribution function from its steady state $\tilde{f}(c)$, quantified here by $(1 - T_{\text{DSMC}}/T_{\text{fit}})$, becomes smaller for smaller dissipation. Consequently, the relaxation of this quantity may be traced only as long as it exceeds the level of natural fluctuations. The smaller the system, the larger is the impact of the fluctuations. Therefore, if the number of particles in the tail is not sufficiently large, the value of $(1 - T_{\text{DSMC}}/T_{\text{fit}})$ drops quickly below the fluctuation level, making an accurate numerical estimate of the relaxation time impossible. This is the case for $\varepsilon = 0.6$ in Fig. 5 where a seemingly fast relaxation is observed due to large fluctuations. Hence, we conclude that the observed relaxation curves do not contradict the predictions of the theory. They indicate, however, that the size of the system of $N = 10^8$ particles is not sufficient to study the relaxation of the distribution function for $\varepsilon = 0.6$ or larger. For a very large system we expect increase of the relaxation time τ_0 with increasing coefficient of restitution ε in agreement with the theoretical analysis.

In summary, we investigated the velocity distribution function of a granular gas and the impact of its overpopulated high-energy tail on the cooling coefficient, which is the main characteristic of a granular gas in the HCS. We proposed a unified functional form of the distribution function that comprises its main part ($v/v_T \equiv c \sim 1$) whose deviation from the Maxwell distribution is described by the second-order Sonine expansion, and the overpopulated tail, which decays exponentially. We derived ε -dependent coefficients of the proposed ansatz along with the scaled velocity c_* , which separates the main part of the velocity distribution ($c \approx 1$) and the tail part ($c \gg 1$). For $\varepsilon \leq 0.7$ the analytical results agree well with large scale DSMC of 10^8 particles, while the deviations for $\varepsilon \geq 0.7$ may be attributed to finite-size effects.

We analyzed the impact of the overpopulated high-energy tail on the cooling rate γ , which is the main hydrodynamic coefficient of granular gases in the HCS. We found systematic deviations from the theoretical expression which neglects the exponential tail. These deviations grow with increasing dissipation (decreasing ε) as $\exp(-6\varepsilon)$, due to enhanced contributions from the tail.

Finally, we observed and explained theoretically the extraordinarily slow (as compared with molecular gases) relaxation of the velocity distribution to its asymptotic stationary form. It takes about ~ 20 – 30 collisions per particle and may be understood from the mechanism of the tail formation.

This research was supported by a grant from the GIF, the German-Israeli Foundation for Scientific Research and Development.

- [1] A. Goldshtein and M. Shapiro, *J. Fluid Mech.* **282**, 75 (1995).
- [2] T. P. C. van Noije and M. H. Ernst, *Granular Matter* **1**, 57 (1998).
- [3] S. E. Esipov and T. Pöschel, *J. Stat. Phys.* **86**, 1385 (1997).
- [4] J. M. Montanero and A. Santos, *Granular Matter* **2**, 53 (1999).
- [5] P. K. Haff, *J. Fluid Mech.* **134**, 401 (1983).
- [6] N. V. Brilliantov and T. Pöschel, *Phys. Rev. E* **61**, 2809 (2000).
- [7] N. V. Brilliantov and T. Pöschel, *Kinetic Theory of Granular Gases* (Oxford University Press, Oxford, 2004).
- [8] J. J. Brey *et al.*, *Phys. Rev. E* **59**, 1256 (1999).
- [9] M. Huthmann *et al.*, *Granular Matter* **2**, 189 (2000).
- [10] W. Losert *et al.*, *Chaos* **9**, 682 (1999).
- [11] F. Rouyer and N. Menon, *Phys. Rev. Lett.* **85**, 3676 (2000).
- [12] J. S. Olafsen and J. S. Urbach, *Phys. Rev. Lett.* **81**, 4369 (1998); *Phys. Rev. E* **60**, R2468 (1999).
- [13] A. Kudrolli *et al.*, *Phys. Rev. Lett.* **78**, 1383 (1997); D. Blair and A. Kudrolli, *Phys. Rev. E* **64**, 050301(R) (2001).
- [14] S. J. Moon *et al.*, *Phys. Rev. E* **69**, 011301 (2004).
- [15] G. A. Bird, *Molecular Gas Dynamics and the Direct Simulation of Gas Flows* (Oxford University Press, Oxford, 1994).
- [16] J. M. Montanero and A. Santos, *Phys. Rev. E* **54**, 438 (1996).
- [17] A. Puglisi *et al.*, *Phys. Rev. E* **59**, 5582 (1999).
- [18] R. Brito and M. H. Ernst, *Europhys. Lett.* **43**, 497 (1998).
- [19] I. Goldhirsch and G. Zanetti, *Phys. Rev. Lett.* **70**, 1619 (1993).
- [20] I. Goldhirsch *et al.*, *Granular Gas Dynamics*, Lecture Notes in Physics, Vol. 624 (Springer, Berlin, 2003), p. 37.
- [21] F. Schurre and G. Kugerl, *Phys. Fluids A* **2**, 609 (1990).
- [22] N. V. Brilliantov and T. Pöschel, *Phys. Rev. E* **61**, 5573 (2000).
- [23] N. V. Brilliantov and T. Pöschel (unpublished).